J Mater Sci: Mater Med (2010) 21:277–282
DOI 10.1007/s10856-009-3843-9

Nanomechanical characterization of tissue engineered bone grown on titanium alloy in vitro

Jinju Chen · M. A. Birch · S. J. Bull

Received: 28 March 2009 / Accepted: 27 July 2009 / Published online: 9 August 2009

Abstract Intensive work has been performed on the characterization of the mechanical properties of mineralised tissues formed in vivo. However, the mechanical properties of bone-like tissue formed in vitro have rarely been characterised. Most research has either focused on compact cortical bone or cancellous bone, whilst leaving woven bone unaddressed. In this study, bone-like mineralised matrix was produced by osteoblasts cultured in vitro on the surface of titanium alloys. The volume of this tissue-engineered bone is so small that the conventional tensile tests or bending tests are implausible. Therefore, nanoindentation techniques which allow the characterization of the test material from the nanoscale to the microscale were adopted. These reveal the apparent elastic modulus and hardness of the calcospherulite crystals (a representative element for woven bone) are 2.35 ± 0.73 and 0.41 ± 0.15 GPa, respectively. The nanoscale viscoelasticity of such woven bone was further assessed by dynamic indentation analysis.

J. Chen (✉) · S. J. Bull
School of Chemical Engineering and Advanced Materials, University of Newcastle, Newcastle Upon Tyne NE1 7RU, UK
e-mail: Jinju.chen82@gmail.com; v.chen@qmul.ac.uk

J. Chen
School of Engineering and Materials Science, Queen Mary University of London, Mile End Road, London E1 4NS, UK

M. A. Birch
Musculoskeletal Research Group Institute for Cellular Medicine, The Medical School, Newcastle University, Newcastle upon Tyne NE2 4HH, UK

1 Introduction

Titanium alloys such as Ti6Al4V are widely used as implant materials in orthopedics due to their excellent biocompatibility, corrosion resistance and low cytotoxcity [1–4]. Their relatively low elastic modulus compared to stainless steel and cobalt chromium alloy also reduces the elastic mismatch between the implant material and the bone thus relieving the stress shielding effect, which can be responsible for potentially damaging resorption of bone on the inner surface of the natural femur.

Most research on the mechanical characterization of bone has focused on material retrieved from animals and humans [5–19]. Various techniques have been used to characterize the mechanical properties of bone such as tensile tests, bending tests, microindentation tests and nanoindentation tests. The majority of the research to date has either focused on cortical bone or cancellous bone, whilst little attention has been paid to woven bone. In this study, immature woven bone was produced on the surface of Ti6Al4V by osteoblasts in vitro. The individual pieces of bone successfully formed on titanium in vitro are typically less than 3 mm in length with a thickness below 50 μm. To assess mechanical properties at such a small scale, nanoindentation techniques are the only viable approach. Nanoindentation techniques can probe mechanical properties at various scales (ranging from nanoscale to microscale) and provide a 'finger print' of the materials response [20, 21]. In order to identify the local structure, a nanoindenter with in situ AFM was used in this study which allows the measurement of local material properties in small, thin and heterogeneous samples which vary significantly due to the localized microstructure (e.g. [22]).

2 Materials and methodology

2.1 Surface topography of the scaffold

Foils and sheets of titanium alloy (Ti6Al4V, Goodfellow) were polished by silicon carbide polishing paper. The samples were then cleaned using ethanol. The surface topography of the titanium alloy (Ti6Al4V) was analyzed by optical profilometry and atomic force microscopy (AFM).

2.2 Cell culture

Sprague-Dawley rat osteoblasts were isolated from the calvariae of 3-day-old neonates by sequential enzymatic digestion as described previously [23]. Cells were then cultured in Dulbecco's modified eagle medium (DMEM) with 100 U/ml Penicilin, 100 μg/ml streptomycin, 2 mM L-Glutamine and 10% (v/v) fetal calf serum (FCS) (all Sigma) at 37°C. Cells were plated onto the surface of the Ti6Al4V at a density of 80,000 cells/ml. The culture media was then exchanged after 48 h to include 5 mM β-glycerophosphate (Sigma), 100 μg/ml L-ascorbic acid phosphate (Wako Ltd) and 10 nM dexamethasone (Sigma) to induce osteoblastic differentiation over a period of 35 days. The osteogenic media was exchanged every 3 days.

2.3 Morphology and composition of the bone

At the end of the culture period, samples were washed twice with PBS and fixed with 4% (w/v) paraformaledhyde in PBS. The mineralised matrix was then stained by Alizarin red staining for better visualisation. The morphology and microstructure of the bone was characterized by environmental scanning electron microscopy (ESEM) and atomic force microscopy (AFM). Energy dispersive X-ray (EDX) was adopted for the chemical composition analysis.

2.4 Nanoindentation

A Hysitron Triboindenter® (Minneapolis, MN, USA) which has excellent load control capability in the μN load range and high spatial resolution (<10 nm) was used to perform the nanoindentation tests. This system has the capability for in situ AFM which is essential to characterize heterogeneous materials such as bone. The surface was scanned prior to the tests and the indenter was carefully located on the calcospherulite crystals or the more mature crystal structures which results from the agglomeration of the calcospherulite crystals. Figure 1 shows the AFM images of the calcospherulite and representative regions

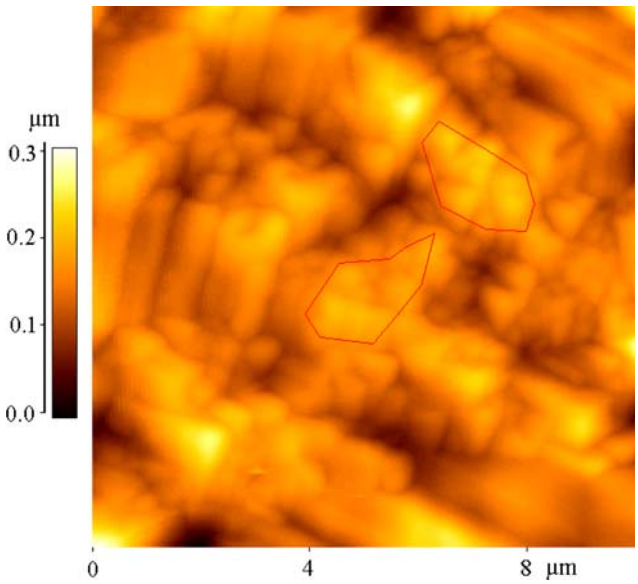

Fig. 1 A representative region of the tissue engineered bone with abundant calcospherulite grains where indents were made

where the indents were located. The average calcospherulite particle is around 800 nm in diameter (which is similar to what is observed in natural bone [24]). As the calcospherulite is a representative element of the bone, it is desirable to maintain the deformation within one grain. To constrain the deformation (at least the plastic deformation) within an individual particle, the penetration should be less than 150 nm. However, at low penetration the surface roughness becomes an issue. To obtain a reasonable evaluation of the elastic modulus or hardness, the penetration should be at least five times bigger than the roughness. The roughness values for the selected regions (e.g. the subregions highlighted in Fig. 1) is 15–20 nm, respectively. Therefore, in this study, a maximum penetration of 100 nm was adopted.

2.4.1 Quasi-static indentation

For materials which may display time-dependent behaviour, displacement control is preferred as is the case in this study. More details about the advantages of displacement control tests can be found in [21, 25, 26]. In this study, the maximum penetration is set at 100 nm with a loading rate of 20 nm/s and a holding period of 5 s at peak load. Around 65 indentation tests were manually performed on selected sample regions.

The elastic modulus and hardness can be determined by the Oliver and Pharr method based on the load-displacement curves generated [27]. For the Poisson's ratio, a value of $\nu = 0.25$ is assumed for the bones tested here.

2.4.2 Dynamic measurement analysis

The Hysitron Triboindenter also features the dynamic measurement analysis mode, which utilizes small amplitude sinusoidal loading concurrent with the quasi-static loading. This is useful to test materials that display viscoelastic behaviour [28]. Three parameters can be directly measured: (1) the *storage modulus*, E': which is related to the elastic properties of the material or the energy recovered after indentation; (2) the *loss modulus*, E'': related to the viscosity of the material or the energy lost during indentation and (3) $tan\delta$: the difference of phase between stress and the strain.

The value of Young's modulus (E) is approximately given by,

$$|E| = \sqrt{E'^2 + E''^2} \quad (1)$$

In this study, the varying dynamic load mode is used and the maximum static load is fixed at 200 μN with loading rate of 40 μN and frequency of 10 Hz. The oscillation load amplitude is 2 μN.

3 Results

3.1 Bone morphology

The surface of the titanium alloy was entirely covered by cells within the first few days. After 7 days, groups of cells had begun to pile up into structures that were the precursor to mineralised matrix deposition (data not shown). After 35 days discrete bone-like nodules were visible to the naked eye on the surface of the titanium alloy substrate. ESEM analysis of the surface (Fig. 2a) reveals that the bone-like matrix has formed. It can be seen that the bone nodules have formed as elongated islands and micropores are present on the bone surface. The spherical shape crystals, the so-called calcospherulite [24] which contain protein, mineral and phospholipids, are also observed in ESEM images (Fig. 2b). EDX analysis of the deposited matrix reveals high concentrations of Ca and P (Fig. 3), which indicate that mineralization has taken place. The measured ratio of Ca/P is 1.67, which agrees with values for hydroxyapatite, the mineral component of bone.

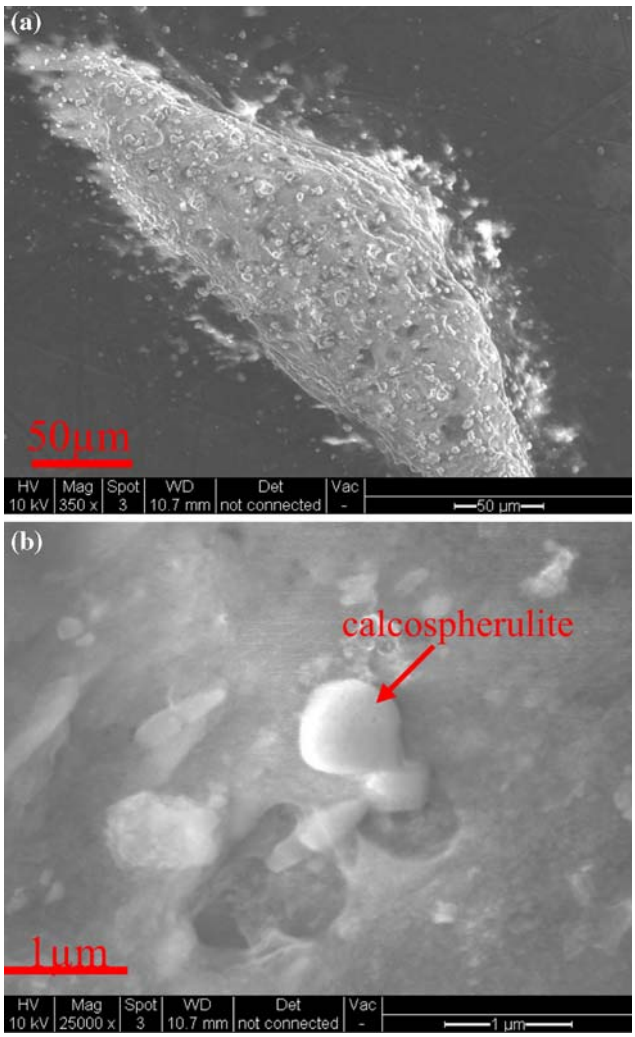

Fig. 2 ESEM images of the tissue engineered bone grown on Ti alloy scaffold for **a** general view and **b** fine microstructure at high magnification

3.2 Nanomechanical properties

3.2.1 Quasi-static nanoindentation analysis

As explained previously, Young's modulus and hardness values were assessed at 100 nm maximum depth under displacement control in this study. Although it is challenging to apply the Oliver and Pharr (O&P) method to materials which show viscoelastic (or viscoplastic) properties, it is still a good approximation if the experimental procedure is well-designed. The average apparent Young's modulus and hardness values obtained by the O&P method are 2.35 ± 0.73, 0.41 ± 0.15 GPa, respectively. The measurement error is standard deviation. As the mineralised matrix has a heterogeneous structure, it is important to know the distribution of the determined values. The statistical distribution of the apparent Young's modulus and hardness values were thus plotted in Fig. 4. It can be seen that the Young's modulus value is most likely to fall within the range of 2 to 2.5 GPa which is slighter higher that that of mineralised pure type 1 collagen derived from a rat tail measured using similar tests [29]. This is a reasonable value compared to what is reported in [30].

In addition to the determination of the elastic modulus and hardness, the recorded load-displacement curve

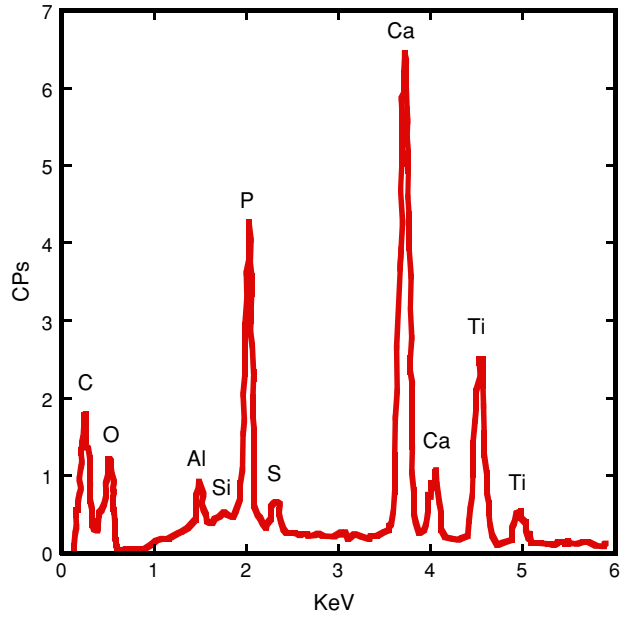

Fig. 3 EDX spectrum of the bone deposited on the titanium alloy scaffold in this study

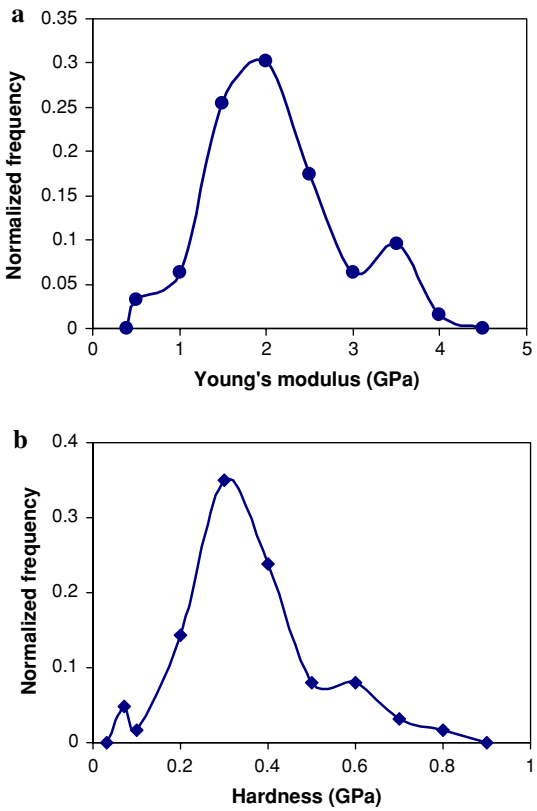

Fig. 4 The statistical distribution of the apparent **a** Young's modulus and **b** hardness determined by the O & P method [27]

associated with the indentation cycle gives a mechanical fingerprint of the indentation history. Figure 5 displays a group of load-displacement curves obtained in a 10 × 10 μm area. All of them show a significant load drop during the holding period which is due to creep or viscoelastic behaviour. Some curves clearly show a surface effect in the initial loading region which is possibly due to the localized surface morphology. Different overall load bearing capacity also results from local composition variations (e.g. the distribution of the protein and mineralization and substructure).

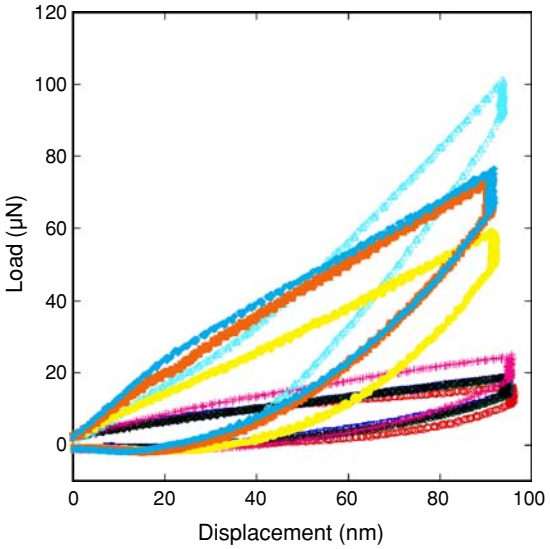

Fig. 5 A group of typical load-displacement curves at 100 nm load control

3.2.2 Dynamic mechanical analysis

Figure 6 displays representative results from the dynamic mechanical measurements performed by the same nanoindenter. An indentation size effect is clearly observed similar to what is reported for natural bone which is due to its heterogenous structure, non-uniform composition and surface roughness [31]. The storage modulus is much bigger than the loss modulus. The Young's modulus from dynamic mechanical analysis (DMA) in the nanoindenter (using Eq. 1) is consistent with what is obtained from the quasi-static indentation tests at 100 nm displacement control in the previous section. The phase difference is around 0.18 which is not negligible. This is supporting evidence of the viscoelasticity of some components within the bone.

4 Discussion

As woven bone contains coarse collagen fibres oriented in an irregular fashion, the mechanical properties of woven bone are more isotropic than those of lamellar bone at the macroscale. Therefore, the anisotropic behaviour well-addressed in the literature for cortical and cancellous bone

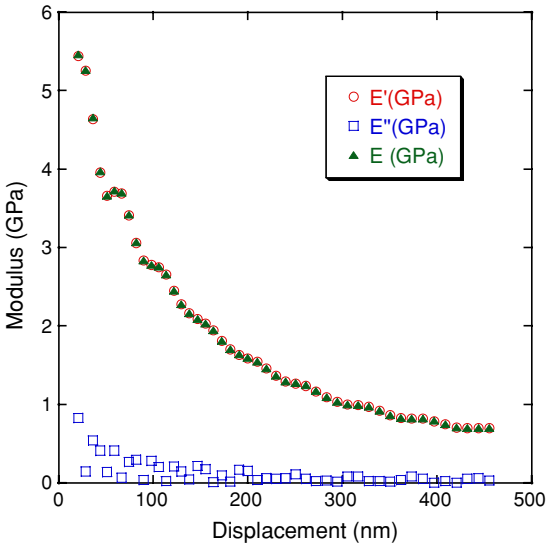

Fig. 6 Elastic modulus, storage modulus, and loss modulus determined by DMA at range of penetration depths

is not a big issue for the woven bone. However, for individual calcospherulite regions, anisotropy may be a factor which affects the histogram of the measured mechanical properties. The determined elastic modulus here is around 8 times higher than that from a femur harvested from a female Sprague-Dawley rat measured by tensile testing [32]. The reason for this is that the tests have been done at dramatically different length scales. In the tensile test, the mechanical response is predominately controlled by the macro/mesoscale structure (such as pore density, ratio of trabecular bone over compact bone, etc.).

The elastic modulus of woven bone in rat fractured callus was reported to be 0.201 ± 0.2 GPa with data spanning from 0.026 to 1.01 GPa for 41 indentations [33]. However, the woven bone measured in [33] is moist which will significantly reduce its stiffness. The localized surface features and indentation size can also contribute to the difference because the maximum penetration used in [33] is over 1000 nm which is much bigger than the 100 nm in this study. Furthermore, the location where the indentation is made in [33] is only selected by reflected light microscopy which is blind to the localized features and microstructure visible by AFM which may account for the big variance in the measured Young's modulus. However, in this study, it was ensured that each individual indentation was made on the calcosperulite crystal structure which is the representative element for dry woven bone. The value of the elastic modulus measured here agrees well with those reported for tissue engineered bone from a similar initial rat osteoblast cell formed on polystyrene (∼2 GPa) and titanium coated polystyrene (∼4 GPa) [30]. The hardness obtained in this study is a few times bigger than the bone formed on polystyrene (∼0.03 GPa) and titanium coated polystyrene (∼0.09 GPa) in vitro [30]. The difference arises from the maturity of the bone due to the different culture conditions and the properties of the substrate. Again, measurement at different length scales is another issue.

It is necessary to point out that the length scale of the current tests (around 100 nm penetration) is commensurate with the dimensions at which individual cells interact with the extracellular environment. Understanding the mechanical properties of bone at this scale is important as it can give us an insight into the likely role that substrate conformity plays in the control of cell behaviour. The elastic modulus and hardness of a surface has been shown to play a crucial role regulating the activity of several cell types [34, 35]. This is achieved through cell—extracellular matrix (ECM) interactions that are of the size to the indentation contact length scale in this study. Bone maturity and the mechanical properties at such length scales may reflect the strength of interaction between the cell and ECM.

5 Conclusions

It was found that bone nodules formed as elongated islands on Ti6Al4V. The bone formed is woven bone as indicated by microstructural analysis. This paper reports the first direct measurement of the mechanical properties of tissue engineered woven bone deposited on a titanium alloy scaffold. It demonstrates that nanoindentation with in situ AFM imaging is very useful to identify and characterise the small features in bone which is not easily achievable by other techniques. The surface topography of sub-regions, heterogeneous microstructure, anisotropy (local grain orientation) and inhomogeneous composition lead to a statistical distribution of the measured Young's modulus and hardness. The average value of the Young's modulus is consistent with what is expected for woven bone in a rat. The hardness values are also reasonable for this type of bone. Dynamic mechanical analysis during nanoindentation can determine the viscoelastic properties of this tissue engineered bone. In this study, it confirms that the cell culture conditions used here yield similar bone structure and Ca/P ratio to natural bone. This is very encouraging and is driving further work on the optimised titanium alloy surface treatment and cell culture conditions for bone growth.

The measured mechanical properties such as elastic modulus and hardness of the bone formed in vitro strongly depend on the length scale, the state of the bone (dehydrated or hydrated), the properties of the scaffold, its composition and localized microstructure. Testing protocols must be used to give contact at similar length scales if comparative studies are to be undertaken.

Acknowledgment Wejie and T.Y. Yang are acknowledged for cell culture. Prof. S. Roy is acknowledged for the help of surface analysis of Ti alloy. Mrs. Pauline Carrick at ACMA is acknowledged for the technical assistance of ESEM and EDX.

References

1. Carr BC, Goswami T. Knee implants–review of models and biomechanics. Mater Des. 2009;30:398–413.
2. Banerjee R, Nag S, Fraser HL. A novel combinatorial approach to the development of beta titanium alloys for orthopaedic implants. Mater Sci Eng C. 2005;25:282–9.
3. Gallardo-Moreno AM, Pacha-Olivenza MA, Saldana L, Perez-Giraldo C, Bruque JM, Vilaboa N, et al. In vitro biocompatibility and bacterial adhesion of physico-chemically modified Ti6Al4V surface by means of UV irradiation. Acta Biomater. 2009;5: 181–92.
4. Lee HU, Jeong YS, Park SY, Jeong SY, Kim HG, Cho CR. Surface properties and cell response of fluoridated hydroxyapatite/TiO2 coated on Ti substrate. Curr Appl Phys. 2009;9:528–33.
5. Boivin G, Bala Y, Doublier A, Farlay D, Ste-Marie LG, Meunier PJ, et al. The role of mineralization and organic matrix in the microhardness of bone tissue from controls and osteoporotic patients. Bone. 2008;43:532–8.
6. Fan Z, Rho JY, Swadener JG. Three-dimensional finite element analysis of the effects of anisotropy on bone mechanical properties measured by nanoindentation. J Mater Res. 2004;19: 114–23.
7. Fan Z, Swadener JG, Rho JY, Roy ME, Pharr GM. Anisotropic properties of human tibial cortical bone as measured by nanoindentation. J Orthoped Res. 2002;4:806–10.
8. Fan Z, Rho JY. Effects of viscoelasticity and time-dependent plasticity on nanoindentation measurements of human cortical bone. J Biomed Mater Res A. 2002;67:208–14.
9. Hengsberger S, Enstroem J, Peyrin F, Nuzzo S, Zysset P. How is the indentation modulus of bone tissue related to its macroscopic elastic response? A validation study. J Biomech. 2003;36:1503–9.
10. Johnson WM, Rapoff AJ. Microindentation in bone: hardness variation with five independent variables. J Mater Sci: Mater Med. 2007;18:591–7.
11. Mullins LP, Bruzzia MS, McHugha PE. Calibration of a constitutive model for the post-yield behaviour of cortical bone. J Mech Behav Biomed Mater. 2009;2:460–70.
12. Lewis G, Xu J, Dunne N, Daly C, Orr J. Evaluation of an accelerated aging medium for acrylic bone cement based on analysis of nanoindentation measurements on laboratory-prepared and retrieved specimens. J Biomed Mater Res B–Appl Biomater. 2007;81:544–50.
13. Oyen ML, Ko CC. Examination of local variations in viscous, elastic, and plastic indentation responses in healing bone. J Mater Sci: Mater Med. 2007;18:623–8.
14. Oyen ML, Ferguson VL, Bembey AK, Bushby AJ, Boyde A. Composite bounds on the elastic modulus of bone. J Biomech. 2008;41:2585–8.
15. Rho JY, Tsui TY, Pharr GM. Elastic properties of human cortical and trabecular lamellar bone measured by nanoindentation. Biomaterials. 1997;18:1325–30.
16. Evans FG. Stress and strain in bone: their relation to fractures and osteogenesis. Springfield, IL: Charles C. Thomas; 1957.
17. Hing KA, Best SM, Tanner KE, Revell PA, Bonfield W. Biomechanical assessment of bone ingrowth in porous hydroxyapatite. J Mater Sci: Mater Med. 1997;8:731–6.
18. Currey JD. The mechanical properties of bone. Clin Orthop Relat Res. 1970;73:210–31.
19. Ascenzi A, Bonucci E, Simkin A. An approach to the mechanical properties of single osteonic lamellae. J Biomech. 1973;6: 227–35.
20. Hainsworth SV, Page TF. Nanoindentation studies of chemomechanical effects in thin-film coated systems. Surf Coat Technol. 1994;68:571–5.
21. Chen J, Bull SJ. Indentation fracture and toughness assessment for thin optical coatings on glass. J Phys D Appl Phys. 2007; 40:5401–17.
22. Chen J, Bull SJ. The investigation of creep of electroplated Sn and Ni–Sn coating on copper at room temperature by nanoindentation. Surf Coat Technol. 2009;203:1609–17.
23. Bokhari MA, Akay G, Zhang SG, Birch MA. The enhancement of osteoblast growth and differentiation in vitro on a peptide hydrogely–polyHIPE polymer hybrid material. Biomaterials. 2005;26:5198–208.
24. Midura RJ, Vasanji A, Su X, Wang A, Midura SB, Gorski JP. Calcospherulites isolated from the mineralization front of bone induce the mineralization of type I collagen. Bone. 2007;41: 1005–16.
25. Warren OL, Wyrobek TJ. Nanomechanical property screening of combinatorial thin-film libraries by nanoindentation. Meas Sci Technol. 2005;16:100–10.
26. Chen J, Bull SJ. Assessment of the toughness of thin coatings using nanoindentation under displacement control. Thin Solid Films. 2006;494:1–7.
27. Oliver WC, Pharr GM. An improved technique for determining hardness and elastic modulus using load and displacement sensing indentation experiments. J Mater Res. 1992;7:1564–83.
28. Syed-Asif SA, Wahl KJ, Colton RJ. Nanoindentation and contact stiffness measurement using force modulation with a capacitive load-displacement transducer. Rev Sci Instrum. 1999;70:2408–13.
29. Chaudhry B, Ashton H, Muhamed A, Yost M, Bull SJ, Frankel D. Nanoscale viscoelastic properties of an aligned collagen scaffold. J Mater Sci: Mater Med. 2009;20:257–63.
30. Saruwatari L, Aita H, Butz F, Nakamura HK, Ouyang J, Yang Y, et al. Osteoblasts generate harder, stiffer, and more delamination-resistant mineralized tissue on titanium than on polystyrene, associated with distinct tissue micro–and ultrastructure. J Bone Miner Res. 2005;20:2002–16.
31. Malzbender J. Comment on "Nanoindentation and whole-bone bending estimates of material properties in bones from senescence accelerated mouse SAMP6". J Biomech. 2005;38:1191–2.
32. Comelekoglu U, Bagis S, Yalin S, Ogenler O, Yildiz A, Ozlen-Sahin N, et al. Biomechanical evaluation in osteoporosis: ovariectomized rat model. Clin Rheumatol. 2007;26:380–4.
33. Leong PL, Morgan EF. Measurement of fracture callus material properties via nanoindentation. Acta Biomater. 2008;4:1569–75.
34. Georges PC, Miller WJ, Meaney DF, Sawyer ES, Janmey PA. Matrices with compliance comparable to that of brain tissue select neuronal over glial growth in mixed cortical cultures. Biophys J. 2006;90:3012–8.
35. Engler AJ, Sen S, Sweeney HL, Discher DE. Matrix elasticity directs stem cell lineage specification. Cell. 2006;126:677–89.